

Uncovering the Role of Ordering in MoSi Superconducting Nanowire Single Photon Detectors with 4D STEM*

G.L. Burton^{1*}, A.E. Lita¹, A.A. Herzing², S.W. Nam¹, and A. Roshko¹

¹National Institute of Standards and Technology, 325 Broadway, Boulder, CO 80305, USA

²National Institute of Standards and Technology, 100 Bureau Dr, Gaithersburg, MD 20899, USA

*Corresponding author: george.burton@nist.gov

Amorphous transition metal-based superconducting nanowires are being explored for a number of critical applications involving single-photon detection for quantum computing, quantum communications, quantum metrology, and deep-space communications. MoSi is a particularly promising material for superconducting nanowire single-photon detectors (SNSPDs) due to their wide range of substrate compatibility and lower superconducting energy gap compared to state of the art polycrystalline NbN and NbTiN. However, significant variations in superconducting transition temperature (T_c) and detection efficiency exist between nanowires processed under slightly different conditions. Here, we explore composition and structure differences between nominally amorphous SNSPD films processed under slightly different conditions with the goal of linking measured differences to device performance.

Samples were prepared by depositing a dielectric SiO₂ spacer layer by plasma-enhanced chemical vapor deposition (PECVD) on 3 inch Si substrates, followed by DC magnetron sputtered MoSi thin films deposited at room temperature and capped with a thin ~2 nm layer of amorphous Si to prevent oxidation [1]. Two different MoSi films were prepared using sputter targets of different Mo:Si ratios (75:25 and 80:20 atomic percent). FIB liftouts were prepared for 4DSTEM measurements taken at 200 kV.

For the sample prepared using a 75:25 sputter target, typical speckled diffraction patterns were recorded (Figure 1c), associated with an amorphous sample. The standard deviation within the first diffraction ring of all diffraction patterns from the same area as Figure 1a was taken to obtain the image in Figure 1b, which shows that some ordering is present. Fluctuation electron microscopy (FEM) variance analysis [2] in Figure 1d was calculated as a function of the scattering vector, $q = 4\pi \sin \theta / \lambda$, following Ref [3]. The sample shows broad peaks mostly associated with the A15 Mo₃Si crystal structure, agreeing well with previous reports [4].

Two different 80:20 samples were analyzed, one showing speckled diffraction patterns similar to the 75:25 sample in Figure 1. However, one of the samples was found to be polycrystalline (see diffraction patterns in Figure 2c-e. An (ABF) image (Figure 2a) was formed by filtering the diffraction patterns with a virtual detector. An agglomerative clustering algorithm with connectivity matrix was applied to find similar diffraction patterns denoted by the different colors in Figure 2b. The device performance of all samples and its relationship to the structure revealed by 4DSTEM and composition revealed by STEM-EDS will be discussed in more detail.

References:

1. Verma, V. B. *et al. Opt. Express, OE* **23**, 33792–33801 (2015).
2. Voyles, P. & Hwang, J. in *Characterization of Materials* 1–7 (2012).

3. Daulton, T.L. *et al.* *Ultramicroscopy* **110**, 1279-1289 (2010).
4. Banerjee, A. *et al.* *Supercond. Sci. Technol.* **30**, 084010 (2017).
5. Contribution of the US Government, not subject to Copyright

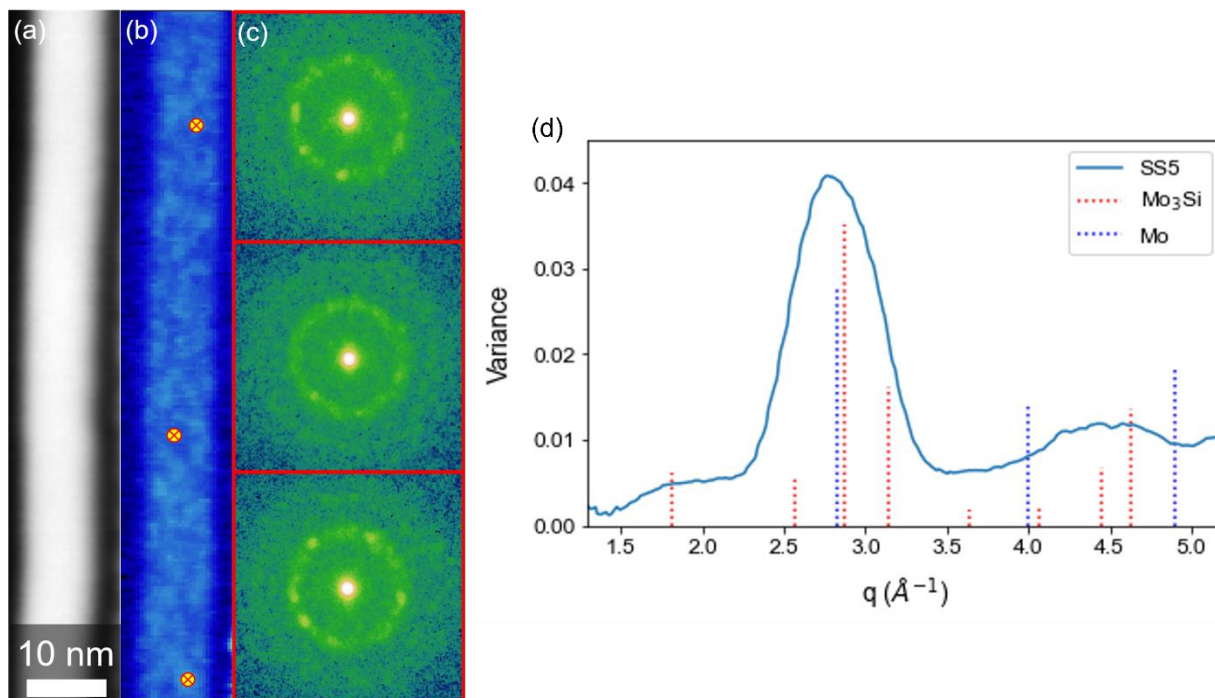


Figure 1. 4DSTEM dataset of a MoSi thin film prepared from a 75:25 sputter target. (a) HAADF image, (b) standard deviation from the first characteristic ring in (c), showing ordered regions, (c) speckled diffraction patterns taken from the nearest cross in (b), and (d) variance calculated from all diffraction patterns in the dataset.

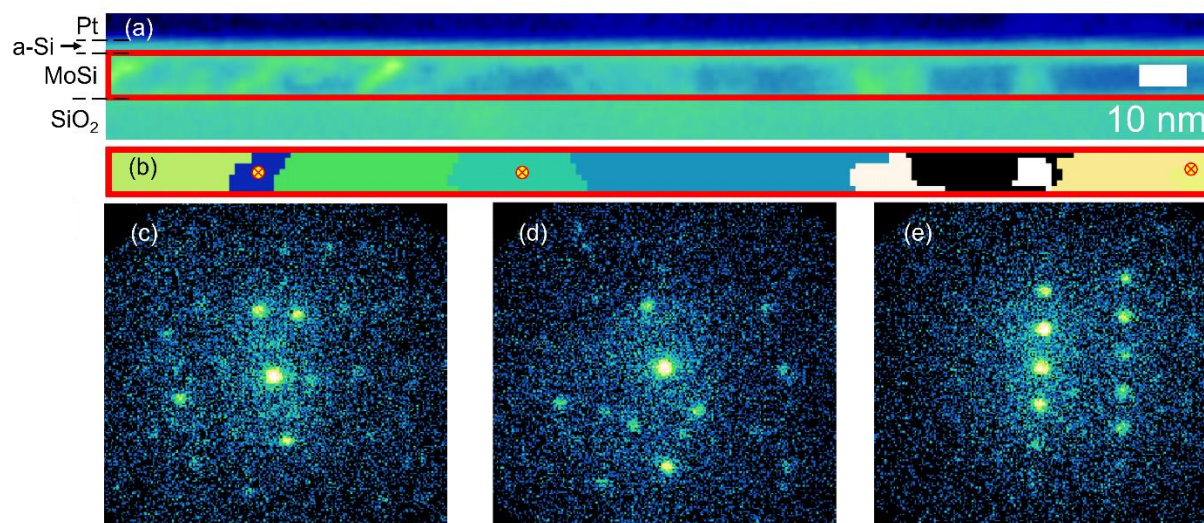


Figure 2. 4DSTEM dataset of a MoSi thin film prepared from an 80:20 sputter target (a) post-processed annular bright field image of the area analyzed, (b) clustering within the MoSi film boxed in red in (a) with regions of similar color denoting similar diffraction patterns and (c)-(d) three diffraction patterns taken from areas denoted by the nearest cross in (b).